International Journal of Advances in Engineering and Management (IJAEM)
Volume 8, Issue 1 Jan. 2026, pp: 309-319 www.ijaem.net ISSN: 2395-5252

Impact of Methane Mass Flow Rate Variations on the Thermal Field of Gas Turbine Combustion Chamber.

[1]Afia, Ephraim R., [2]Akam, Felix N., [3]Philip, Philip E., [4]Inyang, Alphonsus B., ,[5]Bassey, Nsikakabasi I., [6]Kporna, Michael N.,[7]John, John A., [8]Etim, Emmanuel J.,[9] Isaiah, Sylvester B., [10]Umoh, Sifon J.

[1,5] Department of Mechanical Engineering, Federal University of Technology, Ikot Abasi (FUTIA), Akwa Ibom State, Nigeria.
[2] Departmental of Marine Engineering, Akwa Ibom State University, Ikot Akpaden (AKSU), Akwa Ibom State, Nigeria.
[3] Departmental of Mechanical Engineering, Nnamdi Azikiwe University, Awka, Anambra state, Nigeria.
[4] Departmental of Mechanical Engineering, Cross River State University, Cross River State, Nigeria.
[6] Departmental of Mechanical Engineering, University of Warwick, England, United Kingdom.
[7,8] Departmental of Mechanical Engineering, Akwa Ibom State University, Ikot Akpaden (AKSU), Akwa Ibom State, Nigeria.
[9] Department of Electrical Engineering, Federal University of Technology, Ikot Abasi (FUTIA), Akwa Ibom State, Nigeria
[10] Department of Aerospace Engineering, Federal University of Technology, Ikot Abasi (FUTIA), Akwa Ibom State, Nigeria.

Date of Submission: 08-01-2026 Date of Acceptance: 20-01-2026

ABSTRACT:
This computational study investigates the influence of methane fuel mass flow rate on the internal thermal field of a gas turbine Can-Type combustion chamber. A two-dimensional and three-dimensional model of the combustor was developed using AutoCAD and SolidWorks, followed by numerical simulations performed with ANSYS Fluent 2021 R1. The Reynolds-Averaged Navier-Stokes (RANS) equations were solved using the standard k-ε turbulence model, coupled with a one-step eddy dissipation combustion model for methane air reaction. Simulations were conducted across a fuel mass flow rate range of 0.0003 kg/s to 0.0007 kg/s, while maintaining constant inlet air conditions and an adiabatic wall assumption. The results demonstrate a direct but nonlinear relationship between fuel mass flow rate and average combustion chamber temperature. Increasing the fuel flow by 33.3% to 133.33% yielded corresponding temperature increases of only 0.224% to 1.611%, indicating diminishing thermal returns at higher flow rates. Contour plots of static temperature reveal the spatial progression of the high-temperature region with increased fuel input, highlighting intensified thermal loading on chamber walls. The findings underscore the inefficiency of relying solely on increased fuel flow to elevate combustion temperatures beyond a certain threshold. Instead, the study emphasizes the importance of optimizing air-fuel mixing, swirl dynamics, and liner cooling for effective thermal management. This work provides quantified insights that can inform fuel scheduling strategies, combustor design refinement, and cooling system integration to enhance operational efficiency and durability in gas turbine systems. Recommendations for future work include experimental validation and extension of the analysis to alternative fuels and more complex combustion chemistries.

Keywords: *Can Type Combustion Chamber, Mass Flow Rate of Fuel, Gas Turbine, Thermal Analysis, Temperature Field, Computational Fluid Dynamics (CFD), ANSYS Fluent*

I. Introduction

Gas turbines are fundamental to modern power generation and aviation, operating on the Brayton cycle to convert the chemical energy of fuel into mechanical work $[1-2]$. The performance and efficiency of these engines are critically dependent on the complex thermochemical processes occurring within the combustion chamber, or combustor, one of the engine's core components alongside the compressor and turbine [3]. As the core component bridging the compressor and turbine, the combustor must efficiently burn fuel within a high-pressure air stream to deliver a high-temperature, uniform working fluid to the turbine inlet $[4-5]$ .This process must be achieved while minimizing pressure losses, ensuring combustion stability and

International Journal of Advances in Engineering and Management (IJAEM)
Volume 8, Issue 1 Jan. 2026, pp: 309-319 www.ijaem.net ISSN: 2395-5252

completeness, and preserving turbine hardware through controlled temperature profiles.

Extensive research has been dedicated to optimizing combustor performance through various avenues. Prior investigations have systematically examined the influence of combustor geometry [6–8] , the use of alternative working fluids [4],and advanced cooling strategies employing baffles and vortex generation [9] . Furthermore, studies have focused on operational stability, analyzing phenomena such as lean blowout in model combustors [10], and have assessed the impact of inlet air distribution [11], humid air [12], and steam-diluted fuels [13]. Material advancements, such as the application of ceramics [14], fundamental studies on the role of turbulence [15] have also contributed to the body of knowledge aimed at enhancing combustion efficiency and reliability. Despite this comprehensive research landscape, a precise, quantified understanding of a key operational parameter remains under-explored: the direct effect of fuel mass flow rate on the internal thermal field within a methane-fueled combustor. While the relationship between fuel input and general performance is acknowledged, the detailed spatial and temporal temperature response to variations in methane mass flow rate lacks systematic characterization. This gap limits the ability to fine-tune operational strategies for optimal efficiency and emissions control under varying load conditions.

To address this lacuna in the current literature, this study employs CFD to conduct a numerical investigation. The primary objective is to quantify the relationship between methane fuel mass flow rate and the resulting temperature distribution inside a model gas turbine combustion chamber. By simulating a range of fuel mass flow rates, this research aims to elucidate the consequent effects on the internal temperature profile of the gas turbine combustion chamber.

The findings of this work are intended to provide actionable insights for gas turbine design engineers and operators. A clear, quantified correlation between fuel flow and combustion chamber thermal management will inform more precise control algorithms, aid in the design of combustors with wider operational envelopes, and contribute to strategies for improving overall cycle efficiency and reducing thermal stresses on turbine components.

II. Materials and Method

2.1 Materials

2.1.1 Combustion Chamber Material

The super-alloy Inconel 718, which is based on nickel, was selected as the material for the combustion chamber wall because of its exceptional strength and ability to withstand oxidation and corrosion at high temperatures.

2.1.2 Fluid Dynamics Computational Tool

In this study, CFD is utilized for analysis and simulation. During the research process, all relevant boundary conditions and assumptions were taken into consideration.

2.1.3 Use of AutoCAD software

The combustion chamber under consideration was designed using the AutoCAD software.

2.1.4 Data Source and Gathering

The Ibom Power Plant Company, situated in the Ikot Abasi Local Government Area of Akwa Ibom State, Nigeria, provided the data for this study. Data are also obtained from published papers, experimental data from other researchers, and data bases or data logbooks.

2.2 Methods

The following are the methodologies used in this study:

2.2.1 Creating a 3D Model of the Combustion Chamber Geometry:

The Can type combustion chamber design was chosen for this study. Figure 1 shows the geometry of the gas turbine Can-Type combustor chamber. The combustor's dimensions are 220 mm in diameter and 420 mm in the Z direction. Vanes give a whirling velocity component by directing the primary input air. The primary main air inlet has a total surface area of 80 cm^2. Fuel is introduced into the primary air flow by means of fuel inlets, each of which has a surface area of 0.21 cm^2. Twelve port air inlets, each with an area of 1.8 cm^2, are used to introduce the primary air into the combustion chamber. The unburned fuel is completely burned by injecting the secondary air after the primary air. The fuel injector injects 0.2 m of dilution air to regulate the flame temperature and NOx emissions. 0.05 m^2 is the area of the can-type combustor's circular outlet. The CFD model used in this work considers a single Can. This system is composed of the primary burner, combustor wall, secondary air inlet, swirl air inlet, dilution air inlet, and output. Air and natural gas can enter the combustor through a swirl burner.

Dilution air has two purposes, providing the additional air required for complete combustion and cooling the combustion liner, which is normally heated to a high temperature.

It is directed to the surrounding cylinder concurrently with secondary air. To accurately depict the swirl flow prior to fuel-air mixing in the main primary

International Journal of Advances in Engineering and Management (IJAEM)
Volume 8, Issue 1 Jan. 2026, pp: 309-319 www.ijaem.net ISSN: 2395-5252

zone, a swirl burner is also modeled. The liner holes are required to cool the combustion products, to maintain a constant temperature profile at the exit in the dilution zone, and to cool the liner wall configuration. They are also required to supply enough air to the primary zone for full combustion at the selected primary zone equivalency ratio of 1:2. The diameter of the air entrance holes is determined by the required greatest penetration. The effective sizes of the holes were calculated using the following formulae in equations (1), (2) and (3).

$$\frac{\Delta P3-4}{P3} = \frac{143.5 M_h \, T3}{P3^2 \, Cd^2 Ah^2} \quad (1)$$

$$Cd = \frac{k-1}{0.6\sqrt{[4k-k(2-\beta)^2]}} \quad (2)$$

$$k = 1 + 0.64\sqrt{[2\mu^2 + (4\mu^4 + 1.56\mu^2\,(4\beta - \beta^2)]} \quad (3)$$

Where:

Ah is the area of inlet ports.

$\frac{\Delta P3-4}{P3}$ term is taken to be 6%

Cd is given as 0.65.

M_h denotes the mass flow rate through the ports (kg/s)

Solid Works, a modeling program, is used to model the combustor in 3-Dimensions (Figure 1). The end view of a 3D model of a combustion chamber of the Can Type is displayed in Figure 2. As seen in Figure 3, a reduced 2-Dimensional solid model was built and used to produce the computational grid (Meshed) in order to simplify the simulation and cut down on computing time as shown in Figure 4.

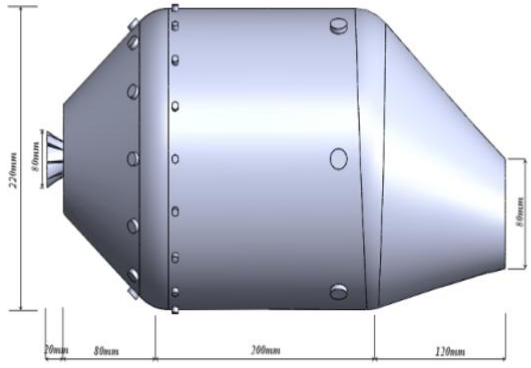

Figure 1: 3D Model of a Can Type Combustion Chamber

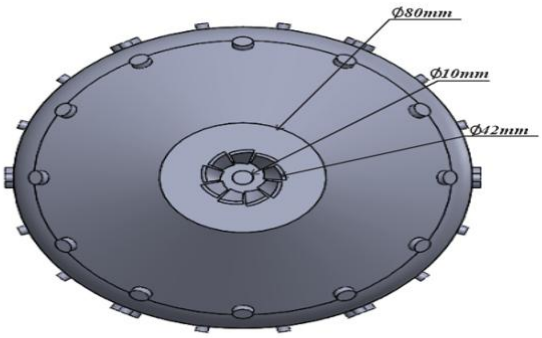

Figure 2: End View of the 3D Model of a Can-Type Combustion Chamber

International Journal of Advances in Engineering and Management (IJAEM)
Volume 8, Issue 1 Jan. 2026, pp: 309-319 www.ijaem.net ISSN: 2395-5252

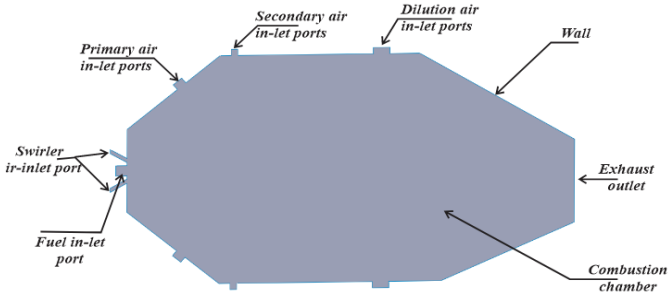

Figure 3: **2D Model of Can Type Combustion Chamber**

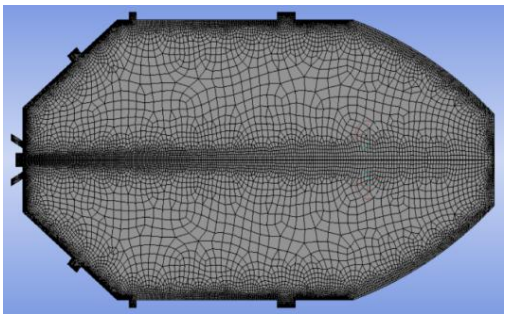

Figure 4: 2D Meshed Model of Can Type Combustion Chamber.

2.2.2 Numerical Requirements for the Research

Table 1: Numerical Requirements for the Research Study.

Inlet boundary conditions

Primary Air	
The injection mass flow rate	0.0012kg/s
Turbulent viscosity ratio	10
Inlet air temperature	633.15K
The turbulence intensity	20%
Mass fraction of oxygen	0.233

Fuel Inlet	
Flow direction	Axial component of flow direction
The injection mass flow rate	0.0003kg/s – 0.0007 kg/s
Turbulent viscosity ratio	10
Inlet fuel temperature	633.15K
The turbulence intensity	20%
The species mass fraction	1
Thermal radiation	Local temperature

Secondary Air	
The injection mass flow rate	0.0018kg/s
Turbulent viscosity ratio	10
Inlet air temperature	633.15K
The turbulence intensity	20%
Mass fraction of oxygen	0.233

Outlet	
The relative pressure	0Pa
Mass fraction of oxygen	0.233
Thermal radiation	Local temperature

Wall	
Wall	Stationary wall
Wall boundary condition	No slip
Wall roughness	Smooth
Wall heat transfer	Adiabatic
Mass sensitivity	0.95
Thermal radiation	Opaque
Diffusion fraction	1

(Author's Compilation)

International Journal of Advances in Engineering and Management (IJAEM)
Volume 8, Issue 1 Jan. 2026, pp: 309-319 www.ijaem.net ISSN: 2395-5252

2.2.3 Mesh Generation

Owing to the combustor's intricate form, an unstructured grid was employed in this investigation. Table 2 provides a summary of the primary quality specifications of the mesh, which was produced automatically. The geometry is intricate, with five distinct solid bodies. Sweep mesh was used, which combines structured and unstructured mesh. Figure 4 shows this in action. In complex geometries, a higher mesh concentration was placed around the burner region to capture important flow development.

Table 2: Mesh parameters

Mesh method	Automatic
Element size	0.02166m
Edge sizing for swirler air inlet port	Number of divisions: 60 Bias factor: 5
Edge sizing for fuel inlet port	Number of divisions: 60 Bias factor: 5
Edge sizing for symmetry axis	Number of divisions: 300 Bias factor: 5
Edge sizing for outlet	Number of divisions: 50 Bias factor: 5
Edge sizing for dilution inlet air	Number of divisions: 60 Bias factor: 5
Edge sizing for secondary inlet air	Number of divisions: 70 Bias factor: 5
Edge sizing for primary inlet air	Number of divisions: 70 Bias factor: 5
Edge sizing for wall	Number of divisions: 140 Bias factor: 5
Growth	1.2
Number of Nodes	14952
Number of Elements	14126
Capture proximity	Yes

(Author's Compilation)

2.2.4 Model Assumptions and the Methane Fuel Combustion Equation

The simplest hydrocarbon, known as an alkane, is methane, an odorless, colorless gas that is found in large quantities in nature or can be produced artificially. It is assumed that the fuel used in this investigation is pure methane. Methane makes up more than 90% of the composition of natural gas; other gas compositions are present, but they are very minor and insignificant. The exothermic (heat-releasing) chemical reaction that takes place when methane is burned. This reaction involves hydrogen, oxygen, and carbon. The following is the reaction's major product list in equation (4), which also includes water, nitrogen oxide, and carbon dioxide:

$$\begin{matrix} CH_4 & + & 4O & \rightarrow & CO_2 & + & 2H_2O & + & Heat \\ (Methane + Oxygen) & \rightarrow & (Carbon\ dioxide & + & water & + & Heat) & & \end{matrix} \quad (4)$$

This indicates that one part of methane must burn for every four parts of oxygen. The combustion reaction's byproduct reveals that there are two parts. As previously mentioned, four oxygen molecules are needed for every methane molecule to completely burn. The volumetric ratio of methane to oxygen is provided in the solution for equation (5) because the oxygen molecule consists of two atoms, or two portions. The generalized eddy-dissipation model is used to investigate the methane-air combustion system. Assuming that the fuel undergoes complete conversion to and, the combustion will be represented by a global one-step reaction mechanism. The reaction is as follows:

$$CH_4 + a(O_2 + 3.76N_2) \rightarrow nCO_2 + \frac{m}{2}H_2O + 3.76\,a\,N_2 + Heat \quad (5)$$

International Journal of Advances in Engineering and Management (IJAEM)
Volume 8, Issue 1 Jan. 2026, pp: 309-319 www.ijaem.net ISSN: 2395-5252

$$n = 1; m = 4$$
$$a = n + \frac{m}{4}$$
$$a = 1 + \frac{4}{4} = 2$$

The overall equation of combustion reaction is given as in equation (6)

$$CH_4 + 2(O_2 + 3.76N_2) \rightarrow CO_2 + \frac{4}{2}H_2O + 3.76\,(2)N_2 + Heat \quad (6)$$

The complete combustion reaction can thus be written as follows in equation (7)

$$CH_4 + 2(O_2 + 3.76N_2) \rightarrow CO_2 + 2H_2O + 7.52\,N_2 + Heat \quad (7)$$
$$(Methane + Oxygen) \rightarrow (Carbon\ dioxide + water + Nitrogen + Heat)$$

The stoichiometric coefficient, formation enthalpies, and reaction rate-controlling factors are defined in terms of the reaction equation above. Using the eddy-dissipation model in the turbulence-chemistry interaction model, the reaction rate will be calculated under the assumption that turbulent mixing is the process that limits the rate.

2.2.5 Determining mass air-fuel ratio for the complete combustion of methane with a 150% theoretical air.

$$CH_4 + 1.5\,x\,2(O_2 + 3.76N_2) \rightarrow CO_2 + 2H_2O + (0.5\,x\,2)O_2 + (1.5x\,7.52)\,N_2 \quad (8)$$

$$Air - fuel\ ratio = \frac{\dot{m}_{air}}{\dot{m}_{fuel}}$$
$$= \frac{1.5\,x\,(2\,x\,4.76)x\,28.97}{1\,x\,(12\,x\,1 + 1\,x\,4)}$$
$$= 25kg\ of\ \frac{air}{kg}of\ fuel$$

2.2.6 Combustion Simulation Process

This study presents a simulation of the combustion process within a gas turbine combustor. The simulation is run using the software ANSYS FLUENT. For the turbulent premixed combustion flame, the ANSYS FLUENT 2021 R1 solver was particularly employed to solve the governing equations. According to the assumptions, the stable Reynolds Average Navier-Stokes (RANS) equations used to describe the air flow and combustion process inside the combustor. Equations (9), (10) and (11) respectively, provide the generic continuity, momentum, and energy equations as follows:

$$\nabla \cdot \left(\rho \vec{V}\right) = 0 \quad (9)$$

$$\frac{\partial}{\partial x_j}\left(\rho u_i\, u_j - \tau_{Ij}\right) = -\frac{\partial P}{\partial x_i}$$
$$\tau_{Ij} = \mu\left(\frac{\partial u_i}{\partial x_j} + \frac{\partial u_j}{\partial x_i}\right) - \frac{2}{3}\mu\frac{\partial u_k}{\partial x_k}\,\delta_{ij} - \bar{\rho}u_i'u_j'$$
$$\nabla \cdot (\rho u_i h) = \nabla \cdot \left(k_{eff}\nabla T\right) + \frac{\partial}{\partial x_j}\left(u_i\,\tau_{Ij}\right) + S_h \quad (10)$$
$$= k + \frac{\mu_t C_p}{Pr_t}$$

$$\frac{\partial(\rho u_j Y_i)}{\partial x_j} = \frac{\partial\left(\rho D\frac{\partial Y_i}{\partial x_j}\right)}{\partial x_j} + M_i\,\omega_i \quad (11)$$

Y_i represents mass fraction for mixture gas of $CH_4, O_2, CO_2, CO, H_2O\ and\ inert\ N_2$. The term $M_i\,\omega_i$ is the mass production rate of species. M_i is the molecular weight of ith species. ω_i is the reaction rate. Gas thermal conductivity, k_t is derived from Prandtl number as in equation (12).

$$\Pr = \frac{\mu C_p}{k_t} \quad (12)$$

Where $\Pr = 0.07$. The diffusion coefficient, D, is estimated by Schmidt number, given as:

$$Sc = \frac{\mu}{D}$$

International Journal of Advances in Engineering and Management (IJAEM)
Volume 8, Issue 1 Jan. 2026, pp: 309-319 www.ijaem.net ISSN: 2395-5252

Where $Sc\ is\ estimated\ as\ 0.7$

2.2.7 Convergence criteria

To define the convergence criteria the following values were considered, thus, for the simulations that used the standard $k-\varepsilon$ model convergence criteria defined can be seen on Table 3.

Table 3: Convergence criteria used on the simulations of the standard $k-\varepsilon$ model.

Residual	Absolute criteria
Continuity	10^{-3}
x-velocity	10^{-3}
y-velocity	10^{-3}
z-velocity	10^{-3}
Energy	10^{-6}
Epsilon	10^{-3}
Fmean	10^{-3}
Fvar	10^{-3}
P1	10^{-6}

(Author's Compilation)

2.2.8 Computing the Temperature Percentage Increase inside the Combustion Chamber

The following formula was used to determine the percentage increase in temperature inside the combustion chamber: (Original temperature - New temperature) / (Original temperature) x 100

Where:

New temperature is the increase temperature inside the combustion chamber.

The initial temperature inside the combustion chamber is known as the original temperature. It is assumed by this formula that the initial temperature was not zero. To prevent division by zero, a separate formula should be applied if the initial temperature is zero.

2.2.9 Temperature Measurement inside the Combustion Chamber

The average temperature inside the combustion chamber during CFD simulations, which are run at different mass flow rates, is used to calculate the temperature inside the chamber. To do this, CFD simulations at various mass flow rates must be run. Temperature data was then extracted from each simulation, the average temperature inside the combustion chamber was determined for each simulation, and the average temperature values were recorded. This method offers a thorough comprehension of the combustion chamber's internal temperature distribution under varied mass flow rates.

III. Results and Discussion

3.1 Relationship between Mass Flow Rate of Methane Fuel and Temperature Inside the Combustion Chamber

Contour plots of static temperature for fuel mass flow rates from 0.0003 kg/s to 0.0007 kg/s are shown in Figures 5-9. The corresponding graph of average temperature versus fuel flow rate is presented in Figure 10.

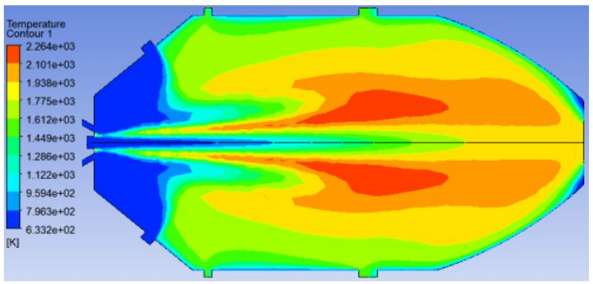

Figure 5: Contour Static Temperature for Combustion with 0.0006kg/s Mass Flow Rate of Methane Fuel

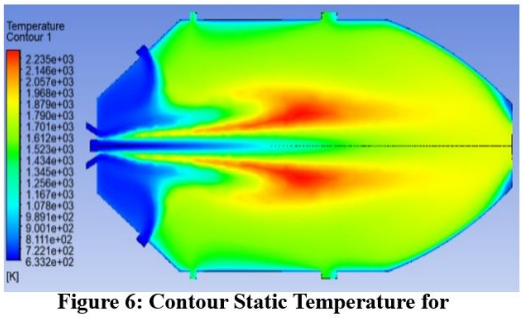

Figure 6: Contour Static Temperature for Combustion with 0.0003kg/S Mass Flow Rate of Methane Fuel

International Journal of Advances in Engineering and Management (IJAEM)
Volume 8, Issue 1 Jan. 2026, pp: 309-319 www.ijaem.net ISSN: 2395-5252

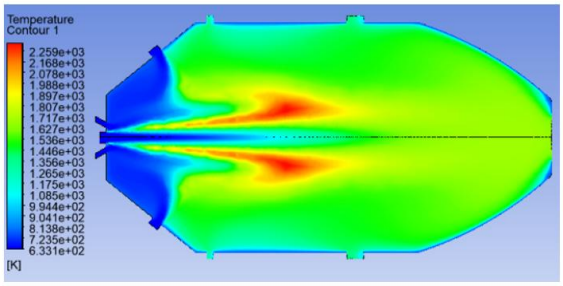

Figure 7: Contour Static Temperature for Combustion with 0.0005 kg/s Mass Flow Rate of Methane Fuel

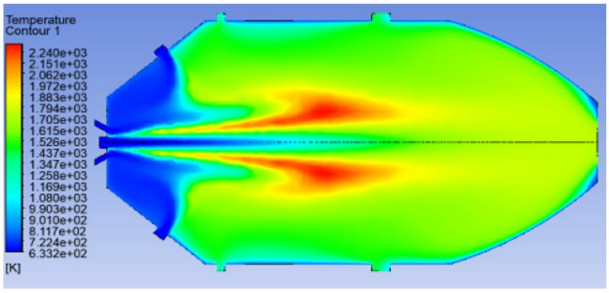

Figure 8: Contour Static Temperature for Combustion with 0.0004 kg/s Mass Flow Rate of Methane Fuel

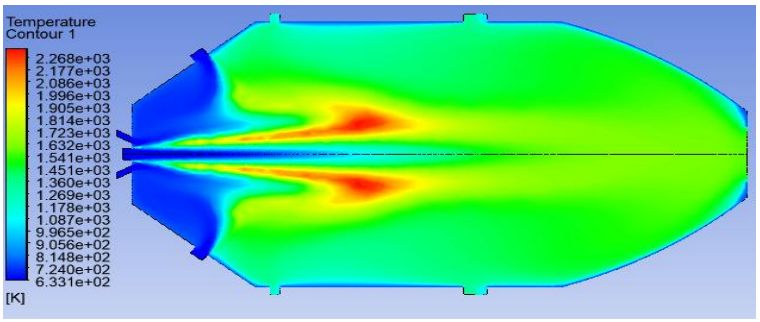

Figure 9: Contour Static Temperature for Combustion with 0.0007 kg/s Mass Flow Rate of Methane Fuel

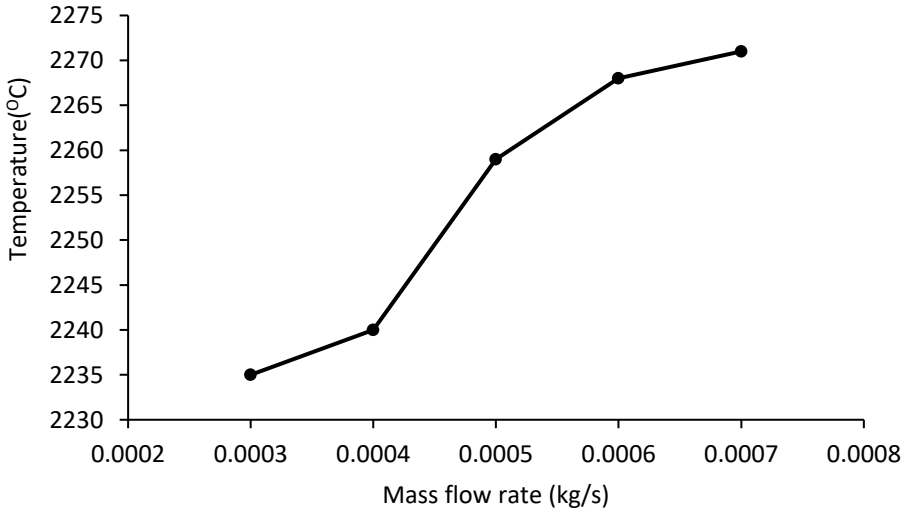

Figure 10: A Graph of Temperature against Mass Flow Rate

The results indicate a direct but nonlinear relationship between methane mass flow rate and the average combustion chamber temperature. As summarized in Table 4, increasing the fuel flow by 33.3% to 133.33% resulted in diminishing returns, with temperature increases of only 0.224% to 1.611%, respectively.

Table 4: Comparison between Percentage Increase in Mass Flow Rate of Fuel and Average Temperature inside the Combustion Chamber.

Range of Mass Flow Rate of Fuel (Kg/S)	Percentage Increase (%)	Range of Average Temperature (^{O}c)	Percentage Increase in Average Temperature (%)

0.0003 – 0.0004	33.33	2235 – 2240	0.224
0.0003 – 0.0005	66.67	2235 – 2259	1.073
0.0003 – 0.0006	100	2235 – 2264	1.477
0.0003 – 0.0007	133.33	2235 – 2268	1.611

The contour plots show the spatial evolution of the high-temperature zone. With increased fuel flow, the high-temperature region expands, leading to intensified thermal loading on the combustor walls. The observed nonlinearity and diminishing thermal returns are attributed to several factors: the fixed air supply limiting complete combustion at higher fuel flows, increased radiative and convective heat losses from the larger flame, and chemical equilibrium limitations at elevated temperatures.

3.2. Comparison with Existing Literature

The finding that geometry and flow organization are critical for thermal management aligns with and extends previous research. Studies focusing on geometric variation [6, 7] established the importance of flow paths.

The present work quantifies how, within a fixed geometry, the control variable of fuel flow has limited thermal efficacy without optimized mixing, reinforcing conclusions from integrated design studies [8]. Furthermore, the diminishing returns highlight why advanced cooling strategies [9] are essential not only for component protection but also for maintaining efficient combustion chemistry at high loads.

3.3. Thermal Implications for Combustor Design

The results demonstrate that simply increasing fuel flow is an inefficient method for raising combustion temperature beyond a certain point. For effective thermal management and performance enhancement, optimization of air-fuel mixing, swirl intensity, and liner cooling is paramount. These insights are directly relevant for improving combustor operability, emissions control, and component durability.

3.4. Limitations of the Study

While this study provides valuable insights, several limitations should be acknowledged:

- **Combustion Chemistry:** The single-step global reaction mechanism does not capture intermediate species, detailed kinetics, or pollutant formation (e.g., NOx).
- **Steady-State Simulation:** The RANS approach does not account for transient phenomena like combustion instabilities or dynamic thermal stresses.
- **Adiabatic Wall Assumption:** Real-world heat transfer through liner cooling was neglected, which would alter the predicted temperature distribution.
- **Modeling Approximations:** The use of the standard k - ϵ model and simplified radiation treatment may not fully capture complex turbulence-chemistry-radiation interactions.
- **Geometry and Boundaries:** The study considered an isolated single can. Interactions in a multi-can array and variations in inlet conditions could influence results.
- **Fuel Composition:** The fuel was assumed to be pure methane, whereas natural gas composition varies.
- **Experimental Validation:** The findings are based solely on numerical simulation and require experimental validation.

Addressing these limitations in future work through advanced modeling, validation, and more detailed physicochemical representations would enhance the predictive capability and practical applicability of the findings.

IV. CONCLUSION AND RECOMMENDATIONS

This computational study has systematically investigated the influence of methane fuel mass flow rate (0.0003 – 0.0007 kg/s) on the thermal field within a Can-Type gas turbine combustion chamber using CFD. The key finding is a direct but nonlinear relationship, where increasing fuel flow by 33.3% to 133.33% yields diminishing temperature rises of only 0.224% to 1.611%.

This nonlinearity underscores the presence of limiting factors such as fixed air supply, increased heat losses, and chemical equilibrium at higher fuel inputs. Spatial analysis confirmed the expansion of the high-temperature core and increased wall thermal loading with higher fuel flow.

The study concludes that relying solely on increased fuel delivery is an inefficient strategy for significantly raising combustion temperatures. Effective thermal management requires integrated

optimization of air-fuel mixing, swirl dynamics, and cooling flows. These quantified insights can inform more precise fuel scheduling algorithms and combustor design for wider operational stability and reduced thermal stress on components.

For further studies, the following are recommended:

- Experimental validation of the computation results.
- Extension of the analysis to transient and off-design conditions.
- Inclusion of detailed chemical kinetics for emission prediction.
- Investigation of the effects of alternative fuel compositions.
- Coupled analysis of thermal and structural performance.

ACKNOWLEDGEMENT

The authors are grateful to all those who in one way or the other contributed to the success of this research.

REFERENCES

[1]. Debey, S., & Neeraj, K. (2015). Study and Analysis of the Effect of Operating Performance Parameter on the Thermal Efficiency of Gas Turbine Power Plan. *International Journal of recent researches in Civil and Mechanical Engineering* IJRRICME, 2(1)213-224, ISSN: 2393- 8471

[2]. Aleksandrov, Y. B. & Mingazov, B.G. (2017). Optimal Design of a Combustion Chamber of Gas Turbine Engine by a Combustion Chamber 1D - 2D Computer Program, *Conference series, materials science and engineering.* 240(1), 845-872. DOI: 10.1088/1757-899

[3]. Gibbson, T.B & Wright, L.G. (2009). A review of materials for gas turbines firing syn gas fuels. Oak Ridge National laboratory.

[4]. Ramsai, C., Tathagata, G., Scrinivasa, R., & Vikas, S. (2019). CFD simulation of Gas Turbine combustion chamber by using FEA technique. *Journal of Engineering Technologies and Innovative Research* (JETIR) 6(1), ISSN 234 – 5162.

[5]. Sadykova, A., Samal, B., Dostiyarov, M., Mikhai, G. Z., & Nurlan, R.K. (2020). The Influence of Turbulence on the efficiency and reliability of Combustion Chamber of the Gas Turbine. Gumarbek Daukeev Almaty University of Power Engineering and Telecommunication.

[6]. Kotzer, C., Laviolette, M., & Alan, W. (2009). Effects of Combustion Chamber Geometry upon Exit temperature profiles. *Journal of Engineering for Gas Turbine and Power*; DOI: 1115/GT2009 – 60156

[7]. Joy, J., Wang, PC. and Yu, S. (2018). Effect of Geometric Modification on flow behavior and Performance of Reverse Flow Combustor. *Proceedings of the Institution of Mechanical Engineers,* Part G, *Journal of Aerospace Engineering*. DOI:10.1177/0954410017752717.

[8]. Nandan K J., Sachin, B. M., & Robit, V. G. (2023). Design and Optimization of Combustion Chamber for Gas Turbine Engine. Department of Aerospace Engineering, Chandigarh University, Punjab, India, doi; 10.20944/preprints 202311.1853.XI

[9]. Arjmandi, H., Amini, R., Ghaffari, A., & Chamkha, A. (2021). Effects of Baffles and Vortex Generators on Cooling Performance of a Gas Turbine Combustion Chamber: Numerical Assessment *Alexandria Engineering Journal,* DOI: 10.1016/j.aej.2021.10.005

[10]. Grohmann, J., Rauch, B., Kathrotia, T., Meier, W. & Aigner, M. (2017). Influence of Single Component Fuels on the Gas Turbine Model Combustor Learn Blow Out *AIAA Journals,* 34 (1), https://doi.org/10.2514/1.836456.

[11]. Vijayakumar, K & David, B.(2021). Study of flow field fluid inside a Can Combustor for Micro Gas Turbine Engine under non reacting flow conditions. *Journal of aerospace technology and management.* http//doi.org/10.1590/jatm. v13.1185

[12]. Maqsood, M., Laviolitte, R., and Woodason, R. (2015). Effect of Inlet Air Distribution on Gas Turbine Combustion Chamber Exit Temperature Profiles. *Journal of the American society of Mechanical engineers*.48(4). https//doi.org/10.1115/GT2015-43365

[13]. Yue, W., Gang X., Chaogwn N., & Yufengi C. (2005). Influence of Humid Air on Gaseous combustion of Gas Turbine. *Conference paper*, DOI: 10.1115/GT2006.68946.

[14]. Yu, l., Yufeng C., Gang Xu, & Huang, W. (2007) "The effects of fuel dilution with steam on Gas Turbine combustor performance *Conference paper,* DOI:101115/GT2007 – 27681.

[15]. Dhatchanamoorthy, C., Mohanraj, M., & Vijayan, R. (2014). Study and Performance Analysis of Gas Turbine Combustion chamber and Improving Combustion Efficiency by using Ceramic Composite Material Coating.

Journal of Engineering material science,
Corpus ID:121412381.